Morphology Development in a Range of Nanometer to Micrometer in Sulfonated Poly(ethylene terephthalate) Ionomer

Chang Hyung Lee,[*] Takashi Inoue,[†] and Jae-Woon Nah[‡]

Department of Medical Devices & Radiation Health, Korea Food and Drug Administration, 5, Nokbeon-dong, Eunpyung-gu, Seoul 122-704, Korea
[†]Department of Organic and Polymeric Materials, Tokyo Institute of Technology, Ookayama, Meguro-ku, Tokyo 152, Japan
[‡]Department of Polymer Science and Engineering, Sunchon National University, Jeonnam 540-742, Korea
Received December 10, 2001

We investigated the effect of ionic component on crystalline morphology development during isothermal annealing in a sodium neutralized sulfonated poly(ethylene terephthalate) ionomer (Ion-PET) by time-resolved small-angle x-ray scattering (TR-SAXS) using synchrotron radiation. At early stage in Ion-PET, SAXS intensity at a low annealing temperature (T_a = 120 ºC) decreased monotonously with scattering angle for a while. Then SAXS profile showed a peak and the peak position progressively moved to wider angles with isothermal annealing time. Finally, the peak intensity decreased, shifting the peak angle to wider angle. It is revealed that ionic aggregates (multiplets structure) of several nm, calculated by Debye-Bueche plot, are formed at early stage. They seem to accelerate the crystallization rate and make fine crystallites without spherulite formation (supported by optical microscopy observation). From decrease of peak intensity in SAXS, it is suggested that new lamellae are inserted between the preformed lamellae so that the concentration of ionic multiplets in amorphous region decreases to lower the electron density difference between lamellar crystal and amorphous region. In addition, analysis on the annealing at a high temperature (T_a = 210 ºC) by optical microscopy, light scattering and transmission electron microscopy shows a formation of spherulite, no ionic aggregates, the retarded crystallization rate and a high level of lamellar orientation.

Keywords : Nano-morphology, PET-ionomer, Crystallization, X-Ray scattering.

Introduction

Ionomers, which are polymers containing a low concentration of charged units along the chain, have been the subject of increasing interest during the past twenty years. Many studies of industrially important ionomers have demonstrated that the physical properties of these materials are strongly dependent on morphological features such as the size, quantity, and distribution of ionic aggregates in the polymer.[1] Semicrystalline ionomers add further complications in assessing the morphology formation, since ionic component may intervene in the morphology formation when the constituent polymer crystallizes, and a complicated morphology will be formed by a cooperative effect of ionic component. Consequently, crystallization is expected to be influenced by ionic component.

In semicrystalline ionomers, the influence of the ionic component on the crystallization have been reported.[2,3] Theses studies have focused on final morphology characterization by spectroscopic observation and crystallization kinetics by differential scanning calorimeter (DSC). However, DSC is not enough for quantitative analysis on morphology development. Further more, ionic aggregates range from angstrom to a few nanometers. Therefore, for a better understand of effect of ionic component on crystalline morphology development ranging from the nanometers level to a few micrometers, one needs the time-resolved small-angle x-ray scattering (TR-SAXS) and time-resolved light scattering (TR-LS) studies.

In this paper, we carried out TR-SAXS and TR-LS studies on the morphology development during isothermal annealing in a sodium neutralized sulfonated poly(ethylene terephthalate) ionomer (Ion-PET) and a pure PET (Homo-PET). In additional, the final morphology is studied by wide-angle x-ray scattering (WAXS), optical microscopy (OM), transmission electron microscopy (TEM) and differential scanning calorimeter (DSC), Then we will discuss on the incorporation of ionic component on crystalline morphology in a range of angstrom to micrometer.

Experimental Section

Materials. Sodium neutralized sulfonated PET modified with 1 mol % of sodium 5-sulfoisophthalate (SSI) were supplied by Toyobo Co., Ltd. ($M_n = 2 \times 10^3$). These samples were synthesized by polycondensation of dimethyl terephthalate, SSI, and excess glycol. Manganese acetate and Sb_2O_3 were used as catalysts. The reaction was carried out at 170-220 ºC for 3 h (ester exchange) and then at 285 ºC for 1 h under vacuum (0.1 mmHg) (polycondensation).

Homo-PET was supplied by Toyobo Co., Ltd. (M_w = 6 ×

[*]To whom correspondence should be addressed. Phone: +82-2-380-1756; Fax: +82-2-351-3726; e-mail: c-hlee@kfda.go.kr

10^3, $M_n = 2 \times 10^3$).

All Ion-PET and Homo-PET pellets used in this study were dried under vacuum (10^{-4} mmHg) at 160 ºC for 16 h to remove water before melt-press.

TR SAXS. The pellets were compression-molded between metal plates at 290 ºC for 4 min. The molded specimen was quickly quenched in water bath to obtain an amorphous specimen. The specimen was then cut into thin stripes (7 mm × 5 mm × 1 mm) and again dried under vacuum at room temperature for 24 h. Then this specimen was used for TR SAXS.

The melt-quenched amorphous specimen was placed in a chamber set at room temperature and then transferred quickly into a hot chamber set at a desired annealing temperature T_a. The isothermal annealing at T_a was investigated by the time-resolved SAXS. The X-ray beam was from synchrotron radiation; beam line 3C2 at Pohang Accelerator Laboratory, Pohang, Korea. The storage ring was operated at an energy level of 2 GeV. The SAXS employs a point-focusing optics with a Si double crystal monochromator followed by a bent cylindrical mirror. The incident beam intensity of 0.149 nm wavelength was monitored by an ionization chamber for the correction of minor decrease of the primary beam intensity during the measurement. The geometry was checked by a chicken tendon collagen, which gives a set of sharp diffraction corresponding to Bragg's spacing of 65.3 nm.

The scattering intensity, I, was corrected for background scattering. Then the scattering intensity by thermal fluctuations was subtracted from the SAXS profile $I(q)$ by evaluating the slope of a $I(q)q^4$ versus q^4 plots[5] at wide scattering vectors q, where q is $(4\pi/\lambda)\sin\theta$, λ and θ being the wavelength and scattering angle, respectively. In order to obtain the invariant Q_{SAXS} (eq. 3), the value of the intercept of an $I(q)q^4$ versus q^4 plot K was used to extrapolate the intensity ($= Kq^{-4}$) to $q = \infty$, whereas $Iq^{-1/2}$ versus q^2 was used to extrapolate the intensity at a small q region to $q = 0$. The correction for smearing effect by the finite cross section of the incident beam was not necessary for the optics of SAXS with point focusing.

TR-LS. Using a light scattering photometer equipped with a CCD (charge-coupled device) camera,[6] the kinetics of phase separation were investigated. A polarized He-Ne gas laser of 632.8 nm wavelength was applied perpendicularly to the film specimen. The scattered light was passed through an analyzer. The crystallization kinetics were studied by TR-LS, employing the H_v geometry with a perpendicular set of the two optical axes.

Microscopy Measurement. For TEM analysis, ultrathin sections were cut with micro-tome from crystallized samples and stained with ruthenium tetraoxide (R_uO_4) in the gas phase. The lamellar morphology was observed under TEM with an accelerator voltage of 100 kV (JEM-100CX, JEOL Ltd.). The texture of crystallite was also observed under an OM.

DSC and WAXS. A Perkin-Elmer DSC-7 equipped with a nitrogen purge was used to study the thermal properties of the Ion-PET and Homo-PET. The heating rate was maintained at 20 ºC/min. The glass transition temperatures T_g's were determined as the midpoint of the step change in the heat flow. Amorphous samples were obtained by quenching from 290 ºC to a liquid-nitrogen bath. The isothermally crystallized samples were prepared by annealing the quenched sample in the hot stage at 120 and 210 ºC for 5 h. All samples weight used in DSC scan was 5 mg. WAXS data, in reflection mode, were collected on a Rigaku wide range goniometer with a graphite crystal focusing monochromator.

Results and Discussion

To discuss crystallization kinetics, we investigated integrated intensity Q_{Hv} in Hv mode (cross-polarization) by TR-LS. Q_{Hv} is proportional to the mean-square optical anisotropy $< \delta^2 >$:[7]

$$Q_{Hv} \propto \langle \delta^2 \rangle = \phi_d \delta_d^2 \tag{1}$$

where $<\phi_d>$ is the volume fraction of crystalline domain and δ_d is the anisotropy of the crystalline domain.

At the early stage of crystallization, Q_{Hv} is assumed to be proportional to the volume fraction of crystallite so that the linear growth rate of crystallite G is given by

$$G \propto d(Q_{Hv})^{1/3}/dt \tag{2}$$

Hence we can estimate G from the initial slope of the time variation of $(Q_{Hv})^{1/3}$ in Figure 1. The values of G estimated by eq 2 are shown as a function of crystallization temperature T_a in Figure 2. Growth rate of the Ion-PET (G_{Ion}) increases with increasing T_a, attains maximum at T_a = 190 ºC and then highly drops down. That is, G_{Ion} was higher than G_{Homo} at low crystallization temperatures ($\leq$ 190 ºC), whereas that was smaller than G_{Homo} at high T_a (>190 ºC). In OM observation, crystalline morphology in Ion-PET was found to be different below and above 190 ºC. Figure 3 shows typical OM micrograms for Ion-PET crystallized at T_a = 120 (a) and 210 ºC (b). Fine crystallites were developed at

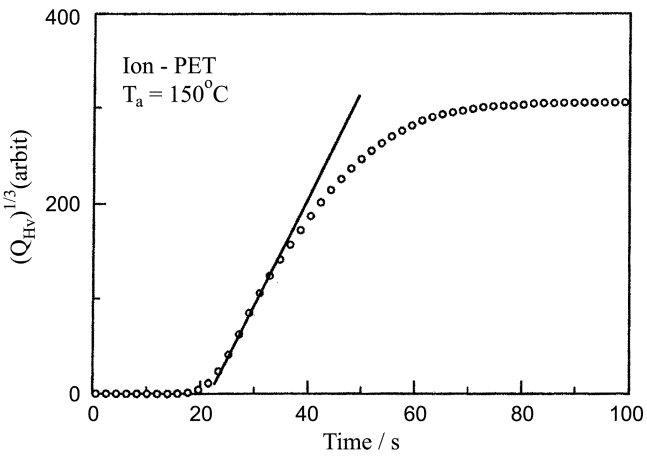

Figure 1. Time variation of the $(Q_{Hv})^{1/3}$.

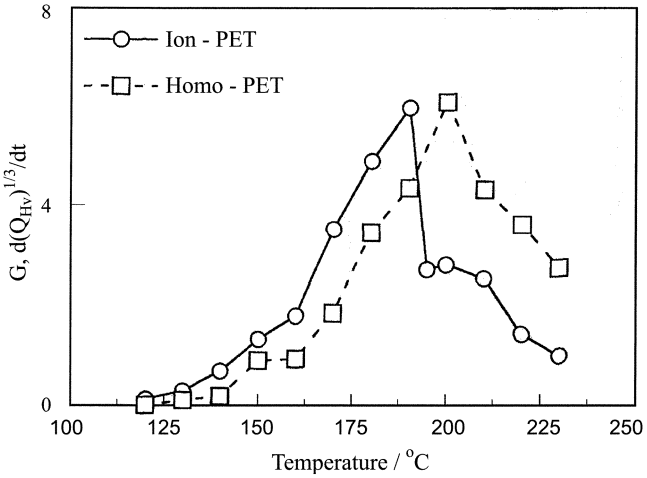

Figure 2. Temperature dependence of the growth rate in a Ion-PET and a Homo-PET.

low T_a (<190 ºC), whereas spherulite structure at high T_a (>190 ºC). Note that Homo-PET showed the spherulite at all T_a's observed. This implies that the crystallization rates can be reduced or accelerated by incorporation of the ionic component for a given crystallization temperature: the ionic component at low temperatures acts as crystalline nucleation agent and accelerates the crystallization rate, whereas that at high temperatures acts as non crystallizable impurity and reduces the crystallization rate. There has been experimental evidence about ionic groups acting as nucleating sites, thereby accelerating the rate of crystallization.[8-10] The higher nucleation densities at low T_a may result in the accelerated crystallization rate and the fine crystallite without highly ordered spherulitic structure.

Figure 4 shows TEM micrographs for Ion-PET annealed at T_a = 120 ºC (a) and 210 ºC (b). In the micrographs, crystalline lamellae appear as white stripes since the staining agent (R_uO_4) penetrates mainly into amorphous regions. The lamellae are arranged multidirectionally and curved so that do not exhibit the ordered structure in larger scale in Figure 4(a), while they are arranged parallel to each other and exhibit the ordered structure in larger scale in Figure 4(b). As shown in Figure 3, the fine crystallites were observed at T_a = 120 ºC, while the spherulite at T_a = 210 ºC. Thus, the fine crystallites are ascribed to the disorder lamellae by incorporation of ionic groups at T_a = 120 ºC, while the spherulite to the ordered structrue of both lamellar bundle and lamellae at T_a = 210 ºC. To clarify effect of the sulfonated component on crystallization in nm level, we investigated the morphology development by TR-SAXS.

Figure 5 shows the time variation of the integrated SAXS intensity, the invariant:

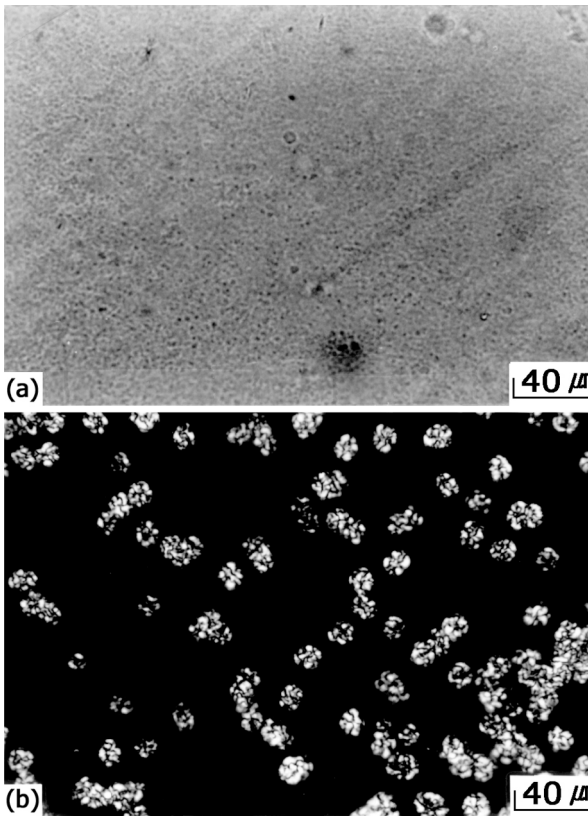

Figure 3. Optical micrographs of a Ion-PET annealed at 120 (a) and 210 ºC (b).

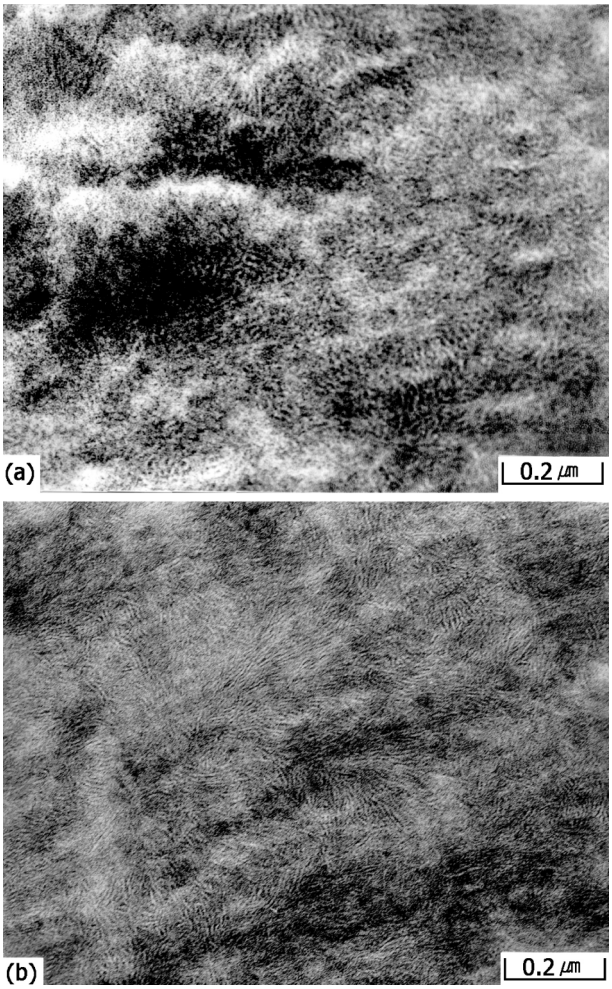

Figure 4. TEM micrographs of a Ion-PET annealed at 120 (a) and 210 ºC (b).

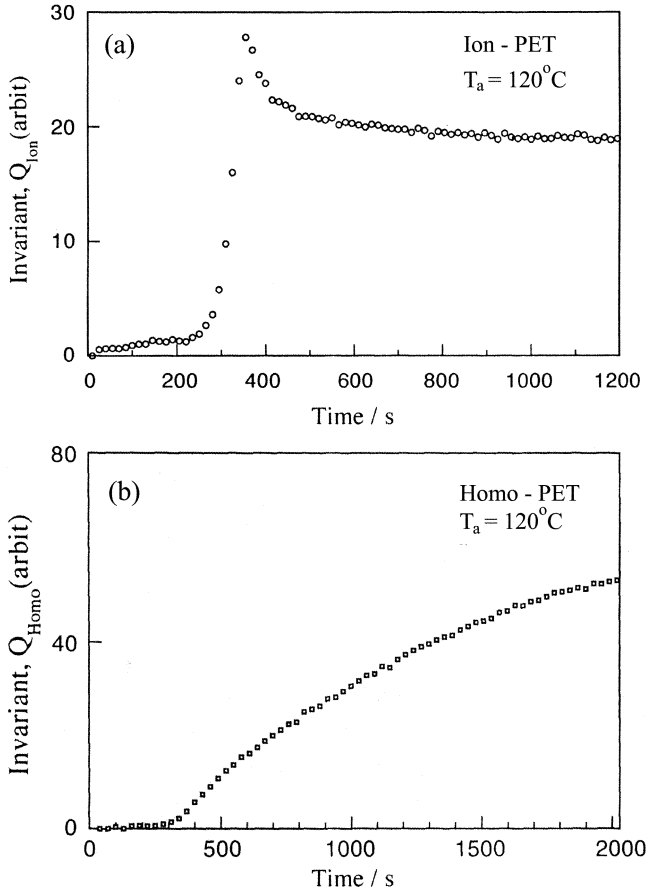

Figure 5. Time variation of the invariant in SAXS: (a) invariant in Ion-PET Q_{Ion} and (b) invariant in Homo-PET Q_{Homo}.

$$Q_{SAXS} = \int_0^\infty q^2 I(q) dq \quad (3)$$

The shape of time variation of Q_{SAXS} in Ion-PET (Q_{Ion}) is completely different from that of Q_{Homo} in Homo-PET. At early stage, Q_{Ion} starts to increase after a short induction period (80s), increases gradually (80s-150s) and keeps constant (150s-210s). Then, that again increases at 210s, attains a maximum, and decreases. Finally, that levels off. The Q_{Homo} starts to increase monotonously after longer induction time and then levels off.

The behavior, keeping Q_{Ion} constant for a while at early stage, is not found in Q_{Homo}. This implies some morphology development before crystallization in Ion-PET. The morphology may be ascribed to ion aggregates, observed often in ionomer.

The model of ionic aggregates is described by Eisenberg *et al.*[12] In their model, a "multiplet" is defined as an aggregate in which the ions are in contact with each other with no intervening hydrocarbon chain. An "ion cluster" is an aggregate of multiplets which exists at high ion contents. As the ion content is increased, ion clusters are preferentially formed and reduce the mobility of the polymer chains. It is known that the sulfonate groups in zinc neutralized sulfonated PET aggregate to form multiplets or lower order clusters in higher ion contents.[13] Multiplets may acts as nucleation

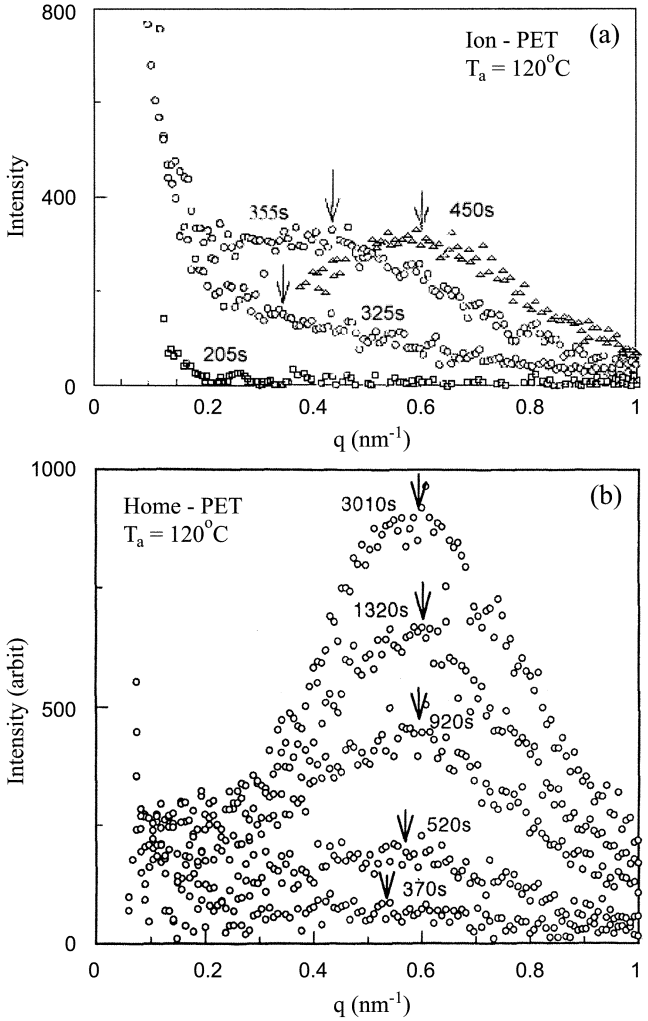

Figure 6. SAXS profiles of a Ion-PET (a) and Homo-PET (b) at various annealing times.

agent and accelerate the rate of crystallization. However, ion clusters may reduce the crystallization rate due to larger contiguous regions of restricted mobility. Actually, the crystallization rate of Ion-PET containing 3 mol % ion was slower than that of both the Homo-PET and the Ion-PET containing 1 mol % ion, implying ion clusters formation. The study on Ion-PET containing 3 mol % ion will be discussed in future paper. On the basis of the above discussion, it is postulated that ionic multiplet structure is formed in the Ion-PET at low temperature, which could explain the increased crystallization rate as compared to that of the Homo-PET. The details of structural development will be discussed by analyzing the SAXS profiles.

Figure 6 compares the SAXS profiles of Ion-PET isothermally annealed at T_a = 120 ºC to that of the Homo-PET. The scattering intensity of an Ion-PET decreases monotonously with q at 205s. Then, the scattering profile shows a peak and the peak position gradually shifts to larger scattering vector with time (325s-355s). The change is accompanied with an increase in the intensity. Finally, the scattering intensity decreases with time, shifting the peak position to

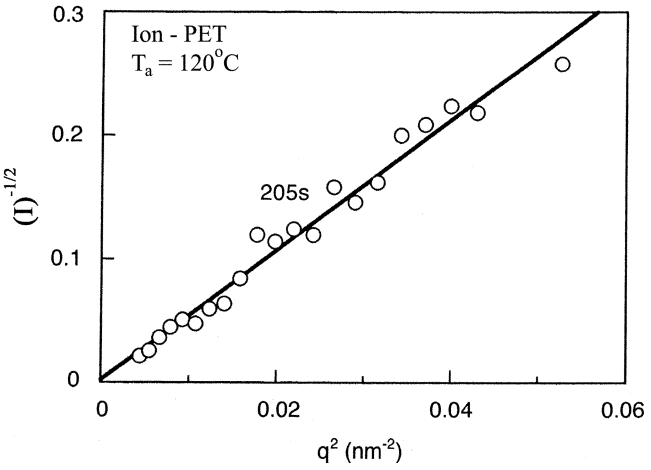

Figure 7. Debye-Bueche plot at annealing time t = 205s.

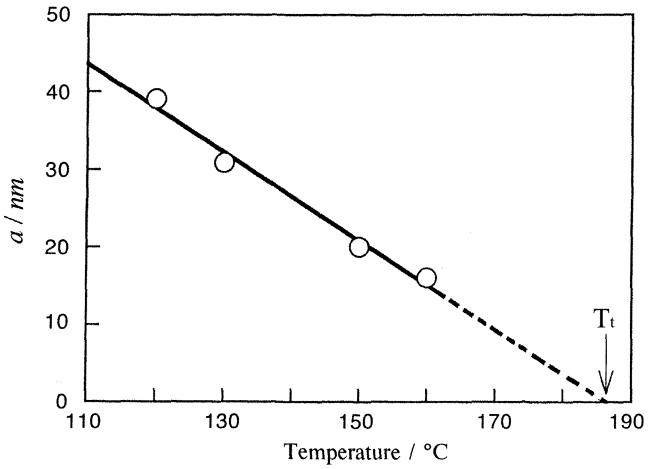

Figure 8. Temperature dependence of the correlation distance *a*.

wider angle (after 355s). The scattering intensity of a Homo-PET exhibits a peak even at early stage, increases with shifting a peak position to wider angle, and then keeps constant.

The scattering intensity of Ion-PET decreases monotonously with scattering angle at early stage, whereas that of Homo-PET exhibits a peak indicative of long period between crystal lamella and amorphous. Thus, the monotonously decreasing scattering profile in Ion-PET could be ascribed to ionic multiplets structure.

As typically shown in Figure 7, the monotonously decreasing scattering profile of Ion-PET at early stage was well described by the Debye-Bueche type scattering function[14,15]

$$I(q) = \left(\frac{1}{A + Bq^2}\right)^2 \tag{4}$$

where A and B are constants (the intercept and slope of Figure 7). One can calculate the correlation distance *a*, given by $(B/A)^{1/2}$ (see eq 4). The typical results of the annealing temperature dependence of *a* are shown in Figure 8. The size of about 40 nm is formed at T_a = 120 ºC and decreased with increasing T_a. A linear decrease of the *a* is seen. An extrapolation of the linear decreasing region to zero correlation distance leads to a temperature of the zero *a* (T_t = 188 ºC). Thus, it is speculated that ionic components form ionic aggregates (multiplets structure) at $T_a < T_t$, whereas these may not form ionic aggregates at $T_a > T_t$. The T_t estimated approximately consists with transition temperature from fine crystallites to spherulite formation (190 ºC), observed by OM. This may be analyzed as follows. At $T_a < T_t$, ionic components form ionic multiplets at early stage, induce high crystalline nucleation, accelerate crystallization rate and develop to yield fine crystallites. On the other hand, at $T_a > T_t$, ionic components without aggregation formation acts as non-crystallizable impurity, retard crystallization and develop to yield spherulite. The absence of ionic aggregates (multiplets) at high temperatures may be ascribed to the very high chain mobility by thermal fluctuation at $T_a > T_t$.

Crystallization kinetics of polymer *G* is described by the Hoffman-Lauritzen theory[16] and is formulated by a combination of the chain mobility term and the nucleation. The chain mobility increases with increasing T_a *i.e.*, (T_a-T_g). The T_g of Homo-PET (78.8 ºC) is approximately identical to that of Ion-PET (79.8 ºC) (see Figure 10(a)). Thus, the accelerated crystallization rate of Ion-PET can be ascribed to the increased nucleation rate due to ionic aggregates, *i.e.* ion multiplets structure. Onset point of the crystallization temperature (122 ºC) in Ion-PET is lower than that of Homo-PET (133 ºC). The shape of crystallization exotherm is sharp for Ion-PET, whereas that broad for Homo-PET. These support that the crystallization rate in Ion-PET is accelerated by ionic aggregates, *i.e.*, multiplets during this DSC scan rate. Regarding the effect of the ionic multiplets, one could discuss in the light of structure analysis for the intermediate and late stage, at which the SAXS scattering peak appears.

The time variation of the intensity at peak position I_m and the long period L_B, given by Bragg's equation $L_B = (2\pi)/q$, is shown in Figure 9. At onset time of crystallization, L_B in Ion-PET (15.7 nm) is larger than that in Homo-PET (13.6 nm). The ionic multiplets dispersed in tens nm order (see Figure 4(a)) and acted as crystalline nucleation agent so that L_B in Ion-PET could be larger than that of Homo-PET at early stage of crystallization.

The time variation of I_m in Ion-PET has a maximum, whereas I_m in Homo-PET gradually increases with time and levels off. The shape of time variation of I_m's in Ion-PET and Homo-PET is similar to that of Q_{Ion} (Figure 5a) and Q_{Homo} (Figure 5b), respectively. Q_{SAXS} can be defined

$$Q_{SAXS} = X_C(1 - X_C)\Delta\rho^2 \tag{6}$$

where X_c is the volume degree of crystallinity, $\Delta\rho$ (= ρ_c-ρ_a) is the difference in the electron density between crystal and amorphous phases. Q_{SAXS} may be expected to attain a maximum and decrease when the value of X_c increases above 0.5 with time: final crystallinity must be higher than

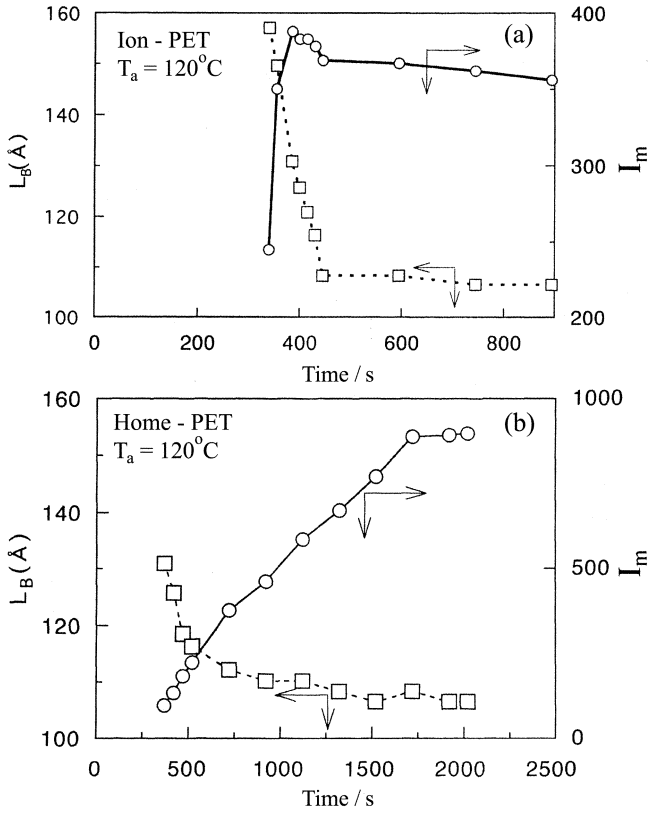

Figure 9. Time variation of the long period L_B and the peak intensity I_m: (a) Ion-PET and (b) Homo-PET.

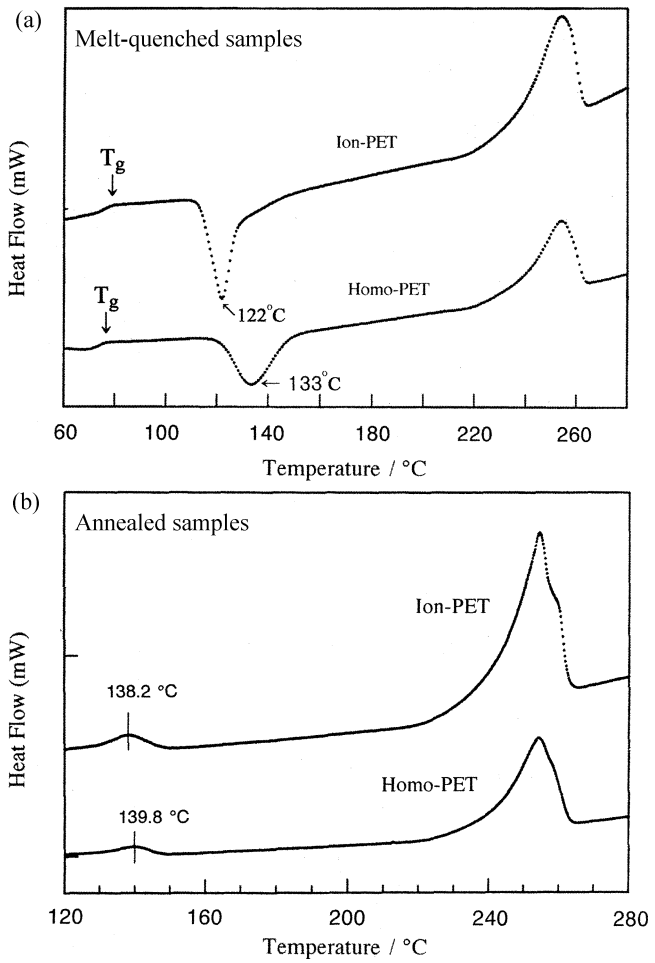

Figure 10. DSC scans: (a) the melt-quenched Ion-PET and Homo-PET; (b) Ion-PET and Homo-PET annealed at T_a = 120 ºC

50%. Q_{Homo} did not show a maximum, whereas Q_{Ion} shows a maximum. If this scenario is reasonable, X_c of Ion-PET should be higher than that of Homo-PET and show the value above 50%. However, crystallinity of Ion-PET is slightly higher than that of Homo-PET as shown in first endothermic area in Figure 10. Note that the degree of crystallinity in Homo-PET, observed at T_a = 120 ºC by Groeninckx *et al.*,[17] is 34%. Thus, a maximum of Q_{Ion} can be ascribed to the change of $\Delta\rho$ during crystallization: new lamellae are inserted between the already existing lamellae so that the concentration of ionic multiplets in amorphous region increase and lower the electron density difference between lamellar crystal and amorphous region. The decrease of $\Delta\rho$ and the increase of X_c ($\leq$ 0.5) are expected to attain a maximum at time variation of Q_{Ion} and I_m as shown in Figures 5(a) and 9(a).

Figures 10(b) shows DSC thermograms for the Ion-PET and Homo-PET both isothermally annealed at T_a = 120 ºC for 6 h. Two endotherms appear at both Ion-PET and Homo-PET. The peak area of the lower temperature endotherm is slightly larger for Ion-PET than for Homo-PET: the degree of crystallinity is slightly higher for Ion-PET. It is seen that ion multiplets slightly increase the degree of crystallinity.

Figure 11 compares the WAXS profile of Homo-PET isothermally annealed at 120 and 210 ºC to that of the Ion-PET. The diffractograms of Ion-PET and Homo-PET crystallized at 120 ºC show three reflection peaks originating from the (010), (î10) and (100) planes, suggesting that both Ion-PET and Homo-PET has the identical polymorphic crystalline structure. However, an increased width of all the reflections as well as a decreased intensity of some of them (*e.g.*, those at (î10) and (100) planes) with respect to the profile of Ion-PET indicates that, due to the corporation of the ionic mutiplets, lower degrees of crystal perfection are obtained.

In Ion-PET annealed at 210 ºC, the reflection shape and peaks is similar to that of the Homo-PET annealed at this temperature, meaning that both Ion-PET and Homo-PET samples have the similar crystal perfection and polymorphic crystal form. This supports indirectly that ionic components do not form aggregates. Note that, at this temperature, the spherulite was observed in both Ion-PET and Homo-PET.

Conclusions

Comparing morphology development and final morphology in Ion-PET with that in Homo-PET, it has been revealed that crystalline morphology is strongly influenced by the incorporation of ionic structure: in Ion-PET crystallized at low temperatures, ionic aggregates (ionic multiplets) appear and, by increasing the crystalline nucleation, they

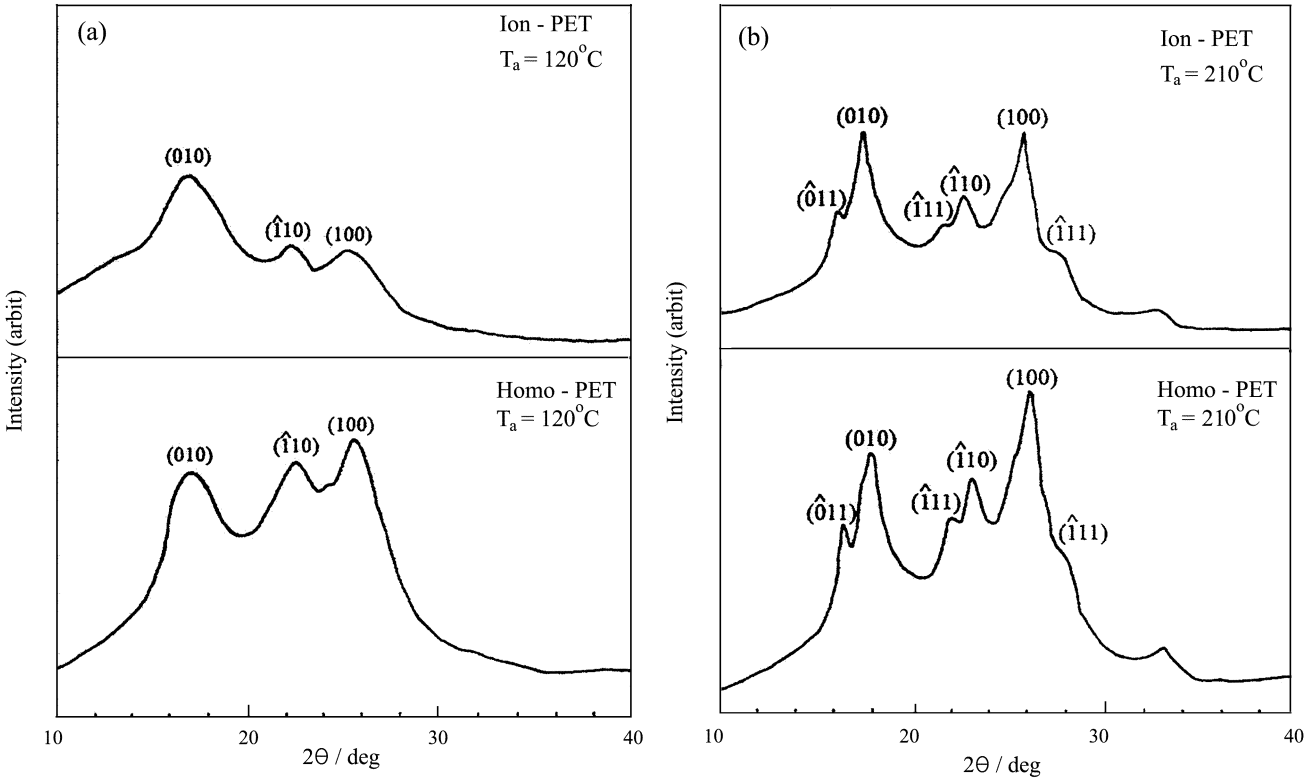

Figure 11. WAXS diffractograms: (a) the Ion-PET and the Homo-PET annealed at 120 ºC; (b) the Ion-PET and the Homo-PET annealed at 210 ºC.

enhance the crystallization rate and develop to yield the fine crystallite without spherulitic superstructure. In addition, these fine crystallites show lower degrees of crystal perfection due to the corporation of the ionic multiplets. In Ion-PET crystallized at high temperature, ionic components form no ionic aggregates and, by acting as non-crystallizable impurity, they reduce the rate of crystallization and develop to yield spherulite. However, the spherulite shows similar crystal perfection to that of the Homo-PET.

Acknowledgment. Synchrotron SAXS experiments were performed at the Pohang Light Source (4C1 beam line) in Korea, which was supported by MOST and Pohang Iron and Steel Co. (POSCO).

References

1. Pineri, M.; Eisenberg, A. *Structure and Properties of Ionomers*; D. Reidel Publishing Company: Dordrecht, Holland, 1987.
2. Bruce Orler, E.; Moore, R. B. *Macromolecules* **1994**, *27*, 4774.
3. Su, Z.; Li, X.; Hsu, S. L. *Macromolecules* **1994**, *27*, 287.
4. Hong, S. M.; Choi, S. H.; Lee, C. H.; Hwang, S. S.; Kim, K. W.; Cho, I. *Polymer J.* **2000**, *32*, 187.
5. Koberstein, J. J.; Morra, B.; Stein, R. S. *J. Appl. Crystallogr.* **1980**, *13*, 34.
6. Lee, C. H.; Saito, H.; Inoue, T. *Macromolecules* **1995**, *28*, 8096.
7. Koberstein, T.; Rusell, T. P.; Stein, R. S. *J. Polym. Sci., Polym. Phys. Ed.* **1979**, *17*, 1719.
8. Legras, R.; Bailly, C.; Daumerie, M.; Dekoninck, J. M.; Mercier, J. P.; Zichy, V.; Nield, E. *Polymer* **1984**, *25*, 835.
9. Mercier, J. P.; Nield, E. *Polymer* **1986**, *27*, 109.
10. Dekoninck, J. M.; Legras, R.; Mercier, J. P. *Polymer* **1989**, *30*, 910.
11. Glatter, O.; Kratky, O. *Small Angle X-ray Scattering*; Academic Press: London, 1982.
12. Eisenberg, A.; Hird, B.; Moore, R. B. *Macromolecules* **1990**, *23*, 4098.
13. Ostrowska-Czubenko, J.; Ostrowska-Gumkowska, B. *Eur. Polym. J.* **1988**, *24*(1), 65.
14. Debye, P.; Bueche, A. M. *J. Appl. Phys.* **1949**, *20*, 518.
15. Debye, P.; Anderson, H. R.; Brumberger, H. J. *J. Appl. Phys.* **1957**, *28*, 679.
16. Lauritzen, J. D.; Hoffman, J. D. *J. Appl. Phys.* **1973**, *44*, 4340.
17. Groeninckx, G.; Reynaers, H.; Berghmans, H.; Smets, G. *J. Polym. Sci., Polym. Phys. Ed.* **1980**, *18*, 1311.